

Transient Weak Protein–Protein Complexes Transfer Heme Across the Cell Wall of *Staphylococcus aureus*

Valerie A. Villareal,^{†,§} Thomas Spirig,[†] Scott A. Robson,^{†,||} Mengyao Liu,[‡] Benfang Lei,[‡] and Robert T. Clubb^{*,†}

[†]Department of Chemistry and Biochemistry and the UCLA-DOE Institute for Genomics and Proteomics, University of California, Los Angeles, California 90095, United States

[‡]Department of Veterinary Biology, Montana State University, Bozeman, Montana 77005, United States

 Supporting Information

ABSTRACT: Iron is an essential nutrient for the bacterial pathogen *Staphylococcus aureus*. Heme in hemoglobin (Hb) is the most abundant source of iron in the human body and during infections is captured by *S. aureus* using iron-regulated surface determinant (Isd) proteins. A central step in this process is the transfer of heme between the cell wall associated IsdA and IsdC hemoproteins. Biochemical evidence indicates that heme is transferred via an activated IsdA:heme:IsdC heme complex. Transfer is rapid and occurs up to 70 000 times faster than indirect mechanisms in which heme is released into the solvent. To gain insight into the mechanism of transfer, we modeled the structure of the complex using NMR paramagnetic relaxation enhancement (PRE) methods. Our results indicate that IsdA and IsdC transfer heme via an ultraweak affinity “handclasp” complex that juxtaposes their respective 3_{10} helices and $\beta 7/\beta 8$ loops. Interestingly, PRE also identified a set of transient complexes that could represent high-energy pre-equilibrium encounter species that form prior to the stereospecific handclasp complex. Targeted amino acid mutagenesis and stopped-flow measurements substantiate the functional relevance of a PRE-derived model, as mutation of interfacial side chains significantly slows the rate of transfer. IsdA and IsdC bind heme using NEAr Transporter (NEAT) domains that are conserved in many species of pathogenic Gram-positive bacteria. Heme transfer in these microbes may also occur through structurally similar transient stereospecific complexes.

Staphylococcus aureus causes a range of life threatening diseases and is a leading cause of lethal hospital- and community-acquired bacterial infections in the United States.¹ The rise of methicillin-resistant *S. aureus* (MRSA) and other multidrug resistant strains has driven efforts to discover novel antibiotics.² One promising therapeutic strategy is to limit microbial access to iron, which is required by *S. aureus* to grow. Heme in hemoglobin (Hb) is the most abundant source of iron in the human body and is captured during infections by *S. aureus* using iron-regulated surface determinant (Isd) proteins.³ The Isd system employs a newly discovered set of cell-wall-attached proteins that first capture Hb on the cell surface and then pass the heme molecule across the cell wall for import into the cytoplasm. The Isd proteins form a network within the cell wall through which heme

is passed via protein–protein complexes; however, the mechanism of heme transfer remains unknown.^{4–6} A central step in heme transfer is the delivery of heme by the IsdA protein to IsdC.⁷ Here we show that the IsdA:heme:IsdC transfer complex forms transiently, and we present a model of its structure derived from NMR paramagnetic relaxation enhancement (PRE) methods.^{8–11} IsdA amino acid mutants that alter residues at the protein–protein interface predicted by the PRE data are impaired in their ability to transfer heme to IsdC, demonstrating that transient, but stereospecific complexes transfer heme after it is removed from Hb.

Stopped-flow measurements indicate that IsdA transfers heme to IsdC > 70 000 times faster than the rate at which IsdA spontaneously releases heme into the solvent.⁷ IsdC binds heme $\sim 10\times$ more tightly than IsdA, suggesting that affinity differences drive the flow of heme from IsdA located on the cell surface to IsdC proteins buried within the cell wall.¹² Kinetic experiments indicate that transfer occurs via an activated IsdA:heme:IsdC complex as the rate of transfer is dependent upon the concentration of IsdC, the heme acceptor (Figure 1A).⁷ IsdC and IsdA bind heme using NEAr Transporter (NEAT) domains that are present in a range of pathogenic Gram-positive bacteria.¹³ In order to investigate the mechanism of transfer, we initially performed conventional NMR chemical shift perturbation experiments that monitored the $^1\text{H}-^{15}\text{N}$ HSQC spectrum of [^{15}N] IsdC^N (residues Ser²⁵ to Gly¹⁵⁰) after adding to it unlabeled IsdA^N (Ser⁵⁸-Lys¹⁸⁸). However, the addition of IsdA^N did not perturb chemical shifts of IsdC^N even when it was present at 3-fold molar excess (data not shown). This finding indicates that IsdA interacts with IsdC with low affinity ($K_d > \sim 5$ mM) and is consistent with our inability to detect interactions between the proteins using affinity-tag pull down experiments (data not shown). Thus, unlike structurally distinct hemophores in Gram-negative pathogens that transfer heme by forming high affinity protein–protein complexes,^{14,15} dramatic increases in the kinetics of heme transfer between NEAT domains are obtained via their transient, weak association.^{7,16}

NMR PRE methods were used to gain insight into the mechanism of heme transfer between IsdA^N and IsdC^N. PRE is the only method capable of probing weak affinity transient-encounter complexes at the atomic level and exploits the large magnetic moment of an unpaired electron present on an attached

Received: April 25, 2011

Published: August 12, 2011

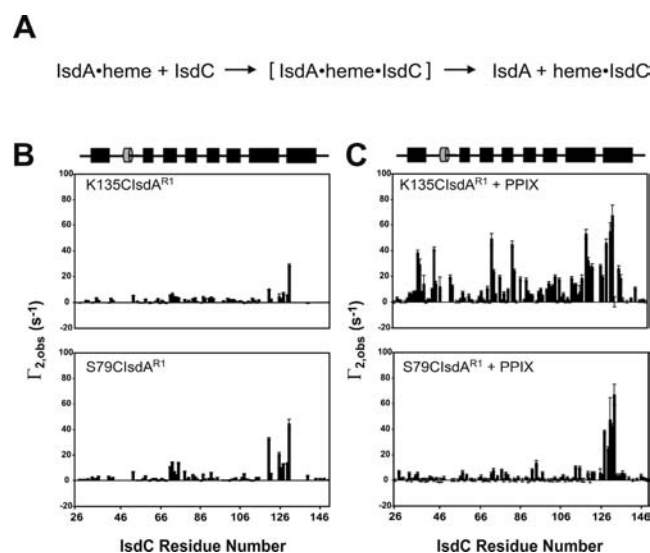


Figure 1. IsdA^{N} and IsdC^{N} weakly associate with one another in the presence of zinc-substituted protoporphyrin (PPIX). (A) Schematic showing the heme transfer reaction from IsdA^{N} to IsdC^{N} . (B) PRE profile of $[\text{}^{15}\text{N}]$ IsdC^{N} in the presence of K135 IsdA^{R1} (top panel) or S79 IsdA^{R1} (bottom panel). No PPIX is present. (C) PRE profile of $[\text{}^{15}\text{N}]$ IsdC^{N} in the presence of PPIX and K135 IsdA^{R1} (top panel) or S79 IsdA^{R1} (bottom panel). In panels (B) and (C), the Γ_2 rates are plotted as a function of IsdC^{N} residue number. Negative Γ_2 rates were set to 0. The secondary structural elements of IsdC^{N} are shown above the profile where the gray cylinder represents the 3_{10} helix and the black bars represent β -strands.

probe.^{8,9,17,18} Two IsdA^{N} single amino acid cysteine mutants containing a disulfide-linked methanethiosulfonate (MTSL)¹⁹ probe were studied: S79C IsdA^{R1} and K135C IsdA^{R1} . The positioning of the probes on IsdA^{N} was chosen so as not to perturb heme binding, and their presence does not alter the kinetics of heme transfer to IsdC^{N} (Supporting Information Figure S1). NMR PRE was measured for complexes containing equal amounts of $[\text{}^{15}\text{N}]$ IsdC^{N} and either S79C IsdA^{R1} or K135C IsdA^{R1} . Experiments were performed in the presence and absence of zinc-substituted protoporphyrin (PPIX), a diamagnetic analogue of heme. The transverse ^1H relaxation rate (R_2) of the amide protons of IsdC^{N} was measured using the two-time point approach for samples of the complex in which the nitroxide probe was either in its paramagnetic or diamagnetic state.²⁰ This enables the determination of Γ_2 , where Γ_2 is proportional to r^{-6} distance between the unpaired electron and the amide proton (Γ_2 is defined as $R_{2\text{para}} - R_{2\text{dia}}$).^{8,9}

Our results indicate that the presence of protoporphyrin triggers the weak association of IsdA^{N} and IsdC^{N} . In the absence of PPIX, the backbone amide hydrogen atoms of IsdC^{N} exhibit only small Γ_2 values when either S79C IsdA^{R1} or K135C IsdA^{R1} is present, suggesting that in the absence of PPIX the proteins do not significantly associate with one another (Figure 1B). However, when the experiment is repeated in the presence of stoichiometric amounts of PPIX, significant increases in Γ_2 are observed presumably as IsdC^{N} and IsdA^{N} associate to transfer PPIX (Figure 1C). The population of the PPIX-dependent complex is extremely low (<5%) as the chemical shifts of IsdC^{N} are unaffected by the addition of IsdA^{N} (Supporting Information Figure S2A). The PPIX-dependent profiles for S79C IsdA^{R1} and K135C IsdA^{R1} also differ substantially (Figure 1C). This is

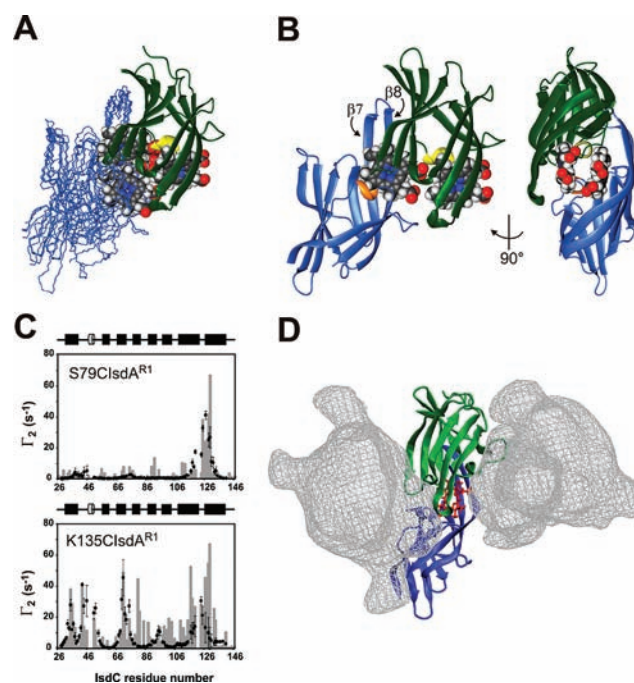


Figure 2. PRE derived models of the transient IsdA^{N} – IsdC^{N} complex. (A) Single conformer representation ($N_e = 1$) of the IsdA^{N} – IsdC^{N} complex. An ensemble of 10 conformers is displayed (IsdA^{N} and IsdC^{N} are colored green and blue, respectively). The backbone atoms of IsdA^{N} have been aligned. All of the conformers in the ensemble interact with one another in a similar manner. (B) A representative ribbon drawing of the complex showing the lowest energy conformer present in the single conformer representation ensemble. Two views are shown. The helices of IsdC^{N} and IsdA^{N} that abut the PPIX are colored orange and yellow, respectively. (C) Comparison of experimental Γ_2 values (gray bars) and back-calculated Γ_2 values (filled circles), which are plotted as a function of residue number, is shown. (D) $N_e = 1 + 3$ multiple conformer representation of the complex with the backbone atoms of IsdA^{N} aligned. Proteins from the $N_e = 1$ representation of the complex are displayed as ribbons, while the multiple representations of IsdC^{N} ($N_e = 3$) are shown as an atomic probability density map.

compatible with the formation of a specific transient protein–protein complex or a set of related complexes. Based on the PRE data, the nitroxide label in K135C IsdA^{R1} is closer to IsdC as it enhances the relaxation of its amide atoms to a greater extent. Importantly, the PPIX-dependent interaction is specific, since in a negative control experiment only small magnitude Γ_2 values are observed in IsdC^{N} after adding a Glu79Cys mutant of small ubiquitin-like modifier protein containing the MTSL probe (Supporting Information Figure S2B).

We used the PRE data and rigid-body simulated annealing refinement to model the structure of the transient IsdA^{N} – IsdC^{N} complex. Structures of the heme bound forms of each protein are known.^{21–23} The protein components were docked so as to simultaneously minimize the difference between the observed and calculated Γ_2 rates using the methodology developed by Clore and colleagues that accounts for the conformational space sampled by the flexible spin label.^{24,25} Initially, the single conformer ($N_e = 1$) approach was used to model data obtained from complexes containing saturating amounts of heme as these conditions yielded larger Γ_2 values. Figure 2A shows an ensemble of structures generated from this procedure that juxtapose the heme binding pockets and satisfy both sets of PRE data to the greatest

extent (overall Q -factor of 0.73 ± 0.01) (Figure 2A and Supporting Information Figure S4A). In the IsdA and IsdC NEAT domains, the heme molecule binds to a hydrophobic cleft located at one end of the β -barrel structure. In the cleft, one face of the protoporphyrin ring lies flat on the surface formed by residues in strands $\beta 7$ and $\beta 8$, while the other side is contacted by a 3_{10} helix. The heme is positioned so as to project the propionate groups into the solvent and the iron is coordinated solely by the phenol ring of a conserved tyrosine residue located in strand $\beta 8$ (Tyr166 and Tyr132 in IsdA^N and IsdC^N, respectively). In all of the docked structures in the ensemble, a “handclasp” orientation is observed in which the loop that connects strands $\beta 7$ and $\beta 8$ ($\beta 7/\beta 8$ loop) on IsdA^N and IsdC^N is positioned adjacent to the 3_{10} helix on the opposing protein (Figure 2B, Supporting Information Table S1 and Figure S3). In this complex, the proteins are pseudosymmetrically related by a twofold rotational axis that is coplanar with the heme molecule and perpendicular to the long axis of the complex. Each heme molecule resides at the molecular interface where it is simultaneously contacted by both proteins, explaining how heme promotes protein association. Interestingly, the positioning of the proteins observed in the complex is generally similar to lattice packing interactions present in crystals of the heme-binding receptor of IsdH (IsdH^{N3}), another NEAT domain hemoreceptor that is located at the bacterial surface.²⁶ This suggests that all heme-binding NEAT domains may be able to transiently associate with one another in a manner similar to the IsdA^N–IsdC^N complex (Supporting Information Figure S3). As shown in Figure 2C, the experimental and back-calculated Γ_2 values show similar profiles indicating that the “handclasp” complex accounts for much of the observed PRE data.

The elevated Q -factors of the IsdA^N–IsdC^N “handclasp” complex indicate that this single structure does not fully account for the PRE data, suggesting that additional encounter complexes exist in solution. An ensemble refinement approach was used to obtain a semiquantitative structural description of encounter interactions between the proteins that may precede or coexist in solution with the stereospecific transfer complex. In this representation, the handclasp complex (which was held fixed) was assumed to be in rapid exchange with an ensemble of three encounter complexes ($N_e = 1 + 3$, where N_e is the number of conformers in the ensemble).²⁴ The inclusion of additional conformers greatly improves the agreement with the PRE data, yielding structures that have an overall Q -factor of 0.26 ± 0.01 (Supporting Information Figure S4B). In the ensemble, a significant fraction of the additional IsdC^N proteins are positioned near both sides of the heme-binding face on IsdA^N, suggesting that they may represent high-energy pre-equilibrium encounter complexes that are poised to relax to the final stereospecific transfer complex (Figure 2D). Ensemble representations that do not contain a fixed complex also fit the PRE data better than the single conformer model (Supporting Information Figures S5 and S6). The activated IsdA:heme:IsdC transfer complex is presumably structurally related to the transient IsdA^N–IsdC^N complex, as similar PRE profiles are observed when saturating or substoichiometric amounts of heme are present.

Heme transfer via a “handclasp”-type complex is mechanistically attractive, as the heme would only need to slide ~ 18 Å from one binding pocket to another and require only minor conformational rearrangements in each protein. Moreover, the heme only needs to undergo a modest rotation as it travels from the donor to the acceptor so as maintain an orientation in which its propionate groups project into the solvent. This is because

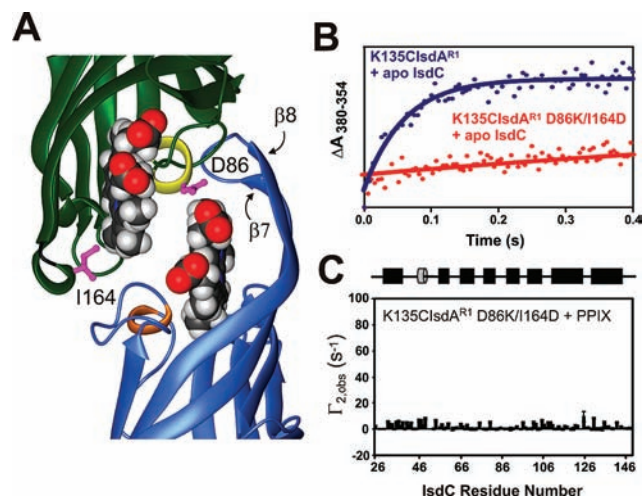


Figure 3. IsdA^N mutations prevent heme transfer to IsdC^N by disrupting transient protein–protein interactions. (A) Close-up image of the binding interface in the stereospecific complex. The side chains of residues in IsdA^N that were mutated to disrupt the interface are shown in magenta (Ile164 in the $\beta 7/\beta 8$ loop and Asp86 in the 3_{10} helix). (B) Disruption of heme transfer from IsdA^N to heme-free IsdC^N. Transfer for K135IsdA^{R1} and the corresponding D86K/I164D mutant was followed using stopped-flow methods measuring spectral changes at 354 and 380 nm as previously described.⁷ (C) PRE profile of [¹⁵N] IsdC^N in the presence of PPIX and K135IsdA^{R1} D86K/I164D. The Γ_2 rates are plotted as a function of IsdC^N residue number. The secondary structural elements of IsdC^N are shown above the profile where the gray cylinder represents the 3_{10} helix and the black bars represent β -strands.

crystallographic studies of the IsdA–heme complex suggest that NEAT domains are capable of binding heme in two distinct orientations in which the heme molecules are related by 180° rotation about the α,γ -meso axis.²¹ To facilitate transfer, IsdC presumably distorts the heme binding pocket of IsdA so as to weaken the axial bond between iron and the phenol group of Tyr166. The specific set of structural changes imparted on IsdA by IsdC cannot be deduced from the PRE data because the transient nature of the complex results in small magnitude Γ_2 rates that have been modeled using rigid-body docking approaches. However, in the stereospecific complex, two IsdA–IsdC contact surfaces surrounding the heme could in principle induce structural distortions in IsdA that promote heme release. On one side of the heme molecule, residues in the turn that connect strands $\beta 7$ to $\beta 8$ in IsdA (P162–I164) are contacted by residues in IsdC immediately following its $\beta 1$ strand (N42–I48) (Supporting Information Figure S3). As strand $\beta 8$ in IsdA houses Tyr166, these interactions could facilitate breakage of the axial bond by displacing the sheet. On the other side of the heme molecule, residues located in the turn connecting strands $\beta 7$ and $\beta 8$ in IsdC (V125 to F130) contact residues following the 3_{10} helix in IsdA (Y87 to K93). This may promote heme release by altering the positioning of the helix which forms stabilizing noncovalent interactions with the heme molecule.

Targeted amino acid mutagenesis and stopped-flow measurements were used to investigate the functional relevance of model of the transfer complex obtained from intermolecular PRE data. Two sites were mutated on IsdA^N: Ile164 in the $\beta 7/\beta 8$ loop and Asp86 in the 3_{10} helix (Figure 3A, Supporting Information Figure S3A). These amino acids were selected because their side chains are positioned at the protein–protein interface in which solvent

accessibility changes by more than 1 \AA^2 (Supporting Information Table S1). Stopped-flow UV–vis measurements are consistent with these residues forming key interactions with IsdC^N during the transfer process as an IsdA^N D86K/I164D double mutant transfers heme to IsdC^N slowly (Figure 3B). This is confirmed by PRE measurements that show the IsdA^N D86K/I164D mutant does not interact with IsdC appreciably (Figure 3C) and heme binding experiments that confirm that the mutant protein binds heme with wild-type affinity (Supporting Information Figure S7). Specific stereochemical interactions likely stabilize the transfer complex as a D86A/I164A double mutant that conservatively alters the same side chains exhibits less pronounced defects in heme transfer (Supporting Information Figure S1).

Combined, these data substantiate the handclasp model of the transfer complex and reveal that the kinetics of heme transfer between IsdA and IsdC can be attenuated by altering potential interactions between their respective $\beta 7/\beta 8$ loops and 3_{10} helices. In conclusion, our results suggest that transient stereospecific complexes can mediate heme transfer between components of the Isd system. Other clinically important Gram-positive pathogens also use structurally related NEAT domains to capture heme on the cell surface (*Streptococcus pyogenes*, *Listeria monocytogenes*, and *Bacillus anthracis*), suggesting that they will also transfer heme via transient protein–protein complexes. The ability to identify functionally relevant interaction surfaces in these ultraweak complexes suggests that small molecules, which disrupt the transfer complex, could serve as antibiotics by limiting microbial access to iron.

■ ASSOCIATED CONTENT

S Supporting Information. Back-calculation of PRE data, control PRE profile, multiple ensemble representations, stopped-flow spectrophotometric data, a description of the materials and methods used, and complete ref 1. This material is available free of charge via the Internet at <http://pubs.acs.org>.

■ AUTHOR INFORMATION

Corresponding Author

*rclubb@mbi.ucla.edu

Present Addresses

^SDepartment of Microbiology and Immunobiology, Harvard Medical School, Boston, Massachusetts 02115, United States.

^{||}Department of Biological Chemistry and Molecular Pharmacology, Harvard Medical School, Boston, Massachusetts 02115, United States.

■ ACKNOWLEDGMENT

We thank Drs. Marius Clore and Charles Schwieters for help with the docking scripts and Dr. Robert Peterson for assistance with the NMR experiments. We would also like to thank Dr. Junji Iwahara for providing data analysis tools and Ms. Sheryll Mangahas for assistance on nitroxide probe attachment. The plasmid encoding the His-tagged SUMO protein was kindly provided by Dr. Feng Guo. This work was supported by NIH Grant AI52217 to R.T.C., NIH Grant RR-020185 to B.L., NIH Training Grant F31GM075564 to V.A.V., and Swiss National Science Foundation Fellowship PBEZP3-124281 to T.S.

■ REFERENCES

(1) Kleven, R. M.; et al. *JAMA, J. Am. Med. Assoc.* **2007**, *298*, 1763–1771.

- (2) Chambers, H. F.; Deleo, F. R. *Nat. Rev. Microbiol.* **2009**, *7*, 629–641.
- (3) Mazmanian, S. K.; Skaar, E. P.; Gaspar, A. H.; Humayun, M.; Gornicki, P.; Jelenska, J.; Joachmiak, A.; Missiakas, D. M.; Schneewind, O. *Science* **2003**, *299*, 906–909.
- (4) Skaar, E. P.; Schneewind, O. *Microbes Infect.* **2004**, *6*, 390–397.
- (5) Maresso, A. W.; Schneewind, O. *Biometals* **2006**, *19*, 193–203.
- (6) Grigg, J. C.; Ukpabi, G.; Gaudin, C. F.; Murphy, M. E. *J. Inorg. Biochem.* **2010**, *104*, 341–348.
- (7) Liu, M.; Tanaka, W. N.; Zhu, H.; Xie, G.; Dooley, D. M.; Lei, B. *J. Biol. Chem.* **2008**, *283*, 6668–6676.
- (8) Clore, G. M. *Protein Sci.* **2011**, *20*, 229–246.
- (9) Clore, G. M.; Iwahara, J. *Chem. Rev.* **2009**, *109*, 4108–4139.
- (10) Bashir, Q.; Scanu, S.; Ubbink, M. *FEBS J* **2011**, *278*, 1391–1400.
- (11) Bashir, Q.; Volkov, A. N.; Ullmann, G. M.; Ubbink, M. *J. Am. Chem. Soc.* **2010**, *132*, 241–247.
- (12) Muryoi, N.; Tiedemann, M. T.; Pluym, M.; Cheung, J.; Heinrichs, D. E.; Stillman, M. J. *J. Biol. Chem.* **2008**, *283*, 28125–28136.
- (13) Andrade, M. A.; Ciccarelli, F. D.; Perez-Iratxeta, C.; Bork, P. *Genome Biology* **2002**, *3*, RESEARCH0047.
- (14) Caillet-Saguy, C.; Piccioli, M.; Turano, P.; Izadi-Pruneyre, N.; Delepierre, M.; Bertini, I.; Lecroisey, A. *J. Am. Chem. Soc.* **2009**, *131*, 1736–1744.
- (15) Krieg, S.; Huche, F.; Diederichs, K.; Izadi-Pruneyre, N.; Lecroisey, A.; Wandersman, C.; Delepierre, P.; Welte, W. *Proc. Natl. Acad. Sci. U.S.A.* **2009**, *106*, 1045–1050.
- (16) Zhu, H.; Xie, G.; Liu, M.; Olson, J. S.; Fabian, M.; Dooley, D. M.; Lei, B. *J. Biol. Chem.* **2008**, *283*, 18450–18460.
- (17) Tang, C.; Iwahara, J.; Clore, G. M. *Nature* **2006**, *444*, 383–386.
- (18) Iwahara, J.; Clore, G. M. *Nature* **2006**, *440*, 1227–1230.
- (19) Battiste, J. L.; Wagner, G. *Biochemistry* **2000**, *39*, 5355–5365.
- (20) Iwahara, J.; Tang, C.; Clore, G. M. *J. Magn. Reson.* **2007**, *184*, 185–195.
- (21) Grigg, J. C.; Vermeiren, C. L.; Heinrichs, D. E.; Murphy, M. E. *Mol. Microbiol.* **2007**, *63*, 139–149.
- (22) Villareal, V. A.; Pilpa, R. M.; Robson, S. A.; Fadeev, E. A.; Clubb, R. T. *J. Biol. Chem.* **2008**, *283*, 31591–31600.
- (23) Sharp, K. H.; Schneider, S.; Cockayne, A.; Paoli, M. *J. Biol. Chem.* **2007**, *282*, 10625–10631.
- (24) Tang, C.; Ghirlando, R.; Clore, G. M. *J. Am. Chem. Soc.* **2008**, *130*, 4048–4056.
- (25) Tang, C.; Louis, J. M.; Aniana, A.; Suh, J. Y.; Clore, G. M. *Nature* **2008**, *455*, 693–696.
- (26) Watanabe, M.; Tanaka, Y.; Suenaga, A.; Kuroda, M.; Yao, M.; Watanabe, N.; Arisaka, F.; Ohta, T.; Tanaka, I.; Tsumoto, K. *J. Biol. Chem.* **2008**, *283*, 28649–28659.